Hindawi Publishing Corporation
Journal of Nanomaterials
Volume 2015, Article ID 413687, 8 pages
http://dx.doi.org/10.1155/2015/413687

Research Article

Theoretical Simulation and Optimization on Material Parameters of Thin Film Bulk Acoustic Resonator

Tao Zhang,[1,2] Fujun Liang,[1] Min Li,[1] Shaorong Li,[1] Huafeng Pang,[1] Sufang Wang,[1] Huaze Zhu,[1] Zhengxin Yan,[1] and Shenggui Zhao[1]

[1] *College of Science, Xi'an University of Science and Technology, Xi'an 710054, China*
[2] *Laboratory of Modern Acoustics, Institute of Acoustics, Nanjing University, Nanjing 210093, China*

Correspondence should be addressed to Tao Zhang; tzhang_psu@yahoo.com

Received 20 June 2015; Accepted 6 September 2015

Academic Editor: Jun Chen

The resonance frequency, f_s, and the effective electromechanical coupling factor, k_{eff}^2, of thin film bulk acoustic resonators (FBARs) are derived by transfer matrix method. The effects of thickness and density of electrode on f_s and k_{eff}^2 with different piezoelectric layers are investigated by numerical calculation method. The results show that thickness and density of electrode affect f_s obviously, especially in large thickness and density area. Moreover, the effects of thickness, density, and acoustic velocity of electrode on k_{eff}^2 of FBAR were also studied. The results show that there is a maximum k_{eff}^2 corresponding to the composition of thickness and density of electrode which is about 20% over the original electromechanical factor of piezoelectric film. k_{eff}^2 is in the direct proportion to the density ρ_e and v_e of electrode, respectively. The electrode thickness affects k_{eff}^2 small with high v_e; moreover, when v_e is high enough, then k_{eff}^2 has almost nothing to do with d_e. k_{eff}^2 always rises with electrode thickness first and then descends with its rising, and the thickness corresponding to the maximum k_{eff}^2 is different with different electrode, but it always locates in the special area. All above results indicate that the thickness, density, and acoustic velocity of electrode are so important that these results can be applied to design FBAR.

1. Introduction

The thin film bulk acoustic resonators (FBARs) are extensively applied for filters, resonators, and sensors, since they were first realized with the resonance frequency of 1.9 GHz in 1999, such as MEMS, biosensors, and gas sensors [1–8]. It is a kind of important device in electronic equipment, and so many kinds of FBARs with high frequency and small dimension have been fabricated during recent ten years for the demand of the industry [9, 10]. The FBARs are especially expected to be investigated and applied by many semiconductor companies such as Agilent, Philip, Murata, and TDK, because of their excellent merits.

Most of researchers focus on the fabrications and the applications of FBAR, and there also are a few researches about numerical simulation and optimization of FBAR. Chao et al. studied the electrode effects of FBAR by Butterworth-van Dyke (BVD) equivalent circuit [11], and Chen and Wang calculated the effective electromechanical coupling coefficient of FBAR [12], and Zhang et al. applied resonant spectrum method to characterize piezoelectric films in FBAR [13]. Besides, our research group published the research about the electrode effect of FBAR [14], and Naumenko analyzed the propagation of acoustic wave in FBAR with Finite Element Method [15], and Kvasov and Tagantsev calculated the nonlinear electrostrictive coefficient with first principles [16]. All of above researches aim at the excellent FBAR performance because the resonance frequency, the effective coupling coefficient, and the accurate optimization for the design of FBAR are the key points for FBAR performance.

As a kind of bulk acoustic resonator (BAR), the figure of merit of an FBAR can be defined by $M = k_{\text{eff}}^2 \cdot Q_S/(1 - k_{\text{eff}}^2)$, and Q_S is the resonance quality factor which is obviously controlled by the piezoelectric layer and electrode effect, and the special research has been done by our research group [14], and so we deeply discuss the material parameter

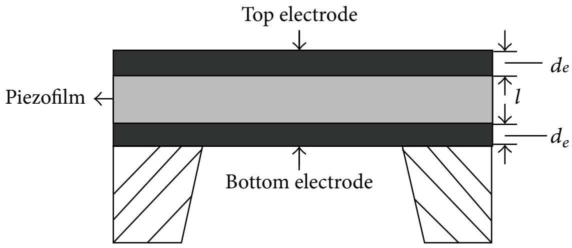

Figure 1: A typical FBAR structure.

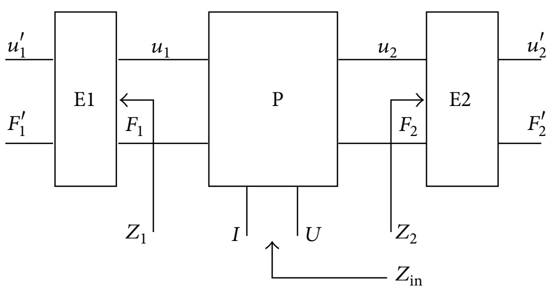

Figure 2: Transfer matrix schematic diagram.

effects of electrode on the resonance frequency, the effective electromechanical coupling factor, and the theoretical optimization consideration of FBAR in this paper considering the regularity among the density ρ_e, the thickness d_e, the acoustic velocity v_e of electrode, and the FBAR performance parameters f_s and k_{eff}^2. The transmission matrix method was used in this research, and the following research points and corresponding simulation results are presented: (1) the transfer matrix method being used to derive the input impedance equation, (2) effects of ρ_e and d_e on f_s, (3) effects of ρ_e and d_e on k_{eff}^2, (4) effects of v_e and d_e on k_{eff}^2, and (5) the two cases with the piezoelectric films of ZnO and AlN, respectively, being compared for discussion.

2. Simulation Method and Procedures

For the FBAR shown in Figure 1, its transfer matrix schematic diagram is shown in Figure 2. P part represents the piezoelectric layer; E1 and E2 parts represent top electrode and bottom electrode, respectively. U and I represent electronic voltage and current port, respectively, F and u represent the force and vibration velocity, respectively, and Z_{in} represents the input acoustic impedance of this system. So we can get the following transfer equation [13]:

$$\begin{bmatrix} U \\ I \end{bmatrix} = [B] \cdot \begin{bmatrix} F \\ u \end{bmatrix}. \quad (1)$$

The piezoelectric transfer matrix $[B]$ can be given as [13]

$$[B] = \frac{1}{\phi H} \begin{bmatrix} 1 & \dfrac{j\phi^2}{\omega C_0} \\ j\omega C_0 & 0 \end{bmatrix} \cdot \begin{bmatrix} \cos\gamma + jZ_E \sin\gamma & Z_0 \left(Z_E \cos\gamma + jZ_E \sin\gamma \right) \\ \dfrac{j \sin\gamma}{Z_0} & 2\left(\cos\gamma - 1\right) + jZ_E \sin\gamma \end{bmatrix}, \quad (2)$$

where $\phi = k_t^2 C_0 Z_0 l / V$ is Mason equivalent circuit transfer ratio, k_t^2 is the electromechanical coupling factor of piezoelectric film, $C_0 = \varepsilon_{33}^S S/l$ is the clamped capacitor with area of S, ε_{33}^S is the dielectric constant with the vertical direction, l is the thickness of piezoelectric film, $Z_0 = \rho VS$ is the acoustic impedance of piezoelectric film with the density of ρ, V is the longitudinal wave velocity, $\gamma = \omega l/V$ is the phase delay in the piezoelectric film, $\omega = 2\pi f$ is angular frequency, and Z_E is the acoustic impedance of electrodes.

We take the electrode material as isotropic, and then we can get the matrix as

$$\begin{bmatrix} F_1 \\ u_1 \end{bmatrix} = \begin{bmatrix} \cos\gamma_{e1} & jZ_{e1}\sin\gamma_{e1} \\ \dfrac{j\sin\gamma_{e1}}{Z_{e1}} & \cos\gamma_{e1} \end{bmatrix} \cdot \begin{bmatrix} F_1' \\ u_1' \end{bmatrix}, \quad (3)$$

where F_1' is zero because of the free top acoustic port, $\gamma_{e1} = \omega l_{e1}/V_{e1}$ is the phase delay in the top electrode, l_{e1} is the thickness of top electrode, V_{e1} is the acoustic velocity of top electrode, $Z_{e1} = \rho_{e1} V_{e1} S$ is the acoustic impedance of top electrode, and ρ_{e1} is the density of top electrode.

We can get Z_1 from (3):

$$Z_1 = \frac{F_0}{u_0} = jZ_{e1} \tan\gamma_{e1}. \quad (4)$$

Similarly, we can get the acoustic impedance of bottom electrode

$$Z_2 = \frac{F_2}{u_2} = jZ_{e2} \tan\gamma_{e2}. \quad (5)$$

So the total input acoustic impedance can be given as [13]

$$Z_{\text{in}} = \frac{U}{I} = \frac{1}{j\omega C_0} \cdot \left[1 - \frac{k_t^2}{\gamma} \cdot \frac{(z_1 + z_2)\cdot\sin\gamma + j\cdot 2\cdot(1-\cos\gamma)}{(z_1+z_2)\cdot\cos\gamma + j\cdot(1 + z_1\cdot z_2)\cdot\sin\gamma} \right]. \quad (6)$$

Inside (6), $z_1 = Z_1/Z_0$, $z_2 = Z_2/Z_0$. We take the top electrode and bottom electrode as the same, so the input impedance (Z_{in}) can be given as (7) with a transfer matrix method [12, 14]

$$Z_{\text{in}} = \frac{1}{j\omega C_0} \left[1 - \frac{k_t^2}{\gamma} \frac{z\sin\gamma + j(1-\cos\gamma)}{z\cos\gamma + (j/2)(1+z^2)\sin\gamma} \right]. \quad (7)$$

$\gamma = \omega l/V$ is the phase shift in the piezofilm, and $z = Z/Z_0$ is the characteristic impedance ratio of the electrodes to the piezofilm as the top and bottom electrodes with the same material and thickness. The series resonance frequency f_s and the parallel resonance frequency f_p can be obtained by (7), and then the effective electromechanical coupling factor of FBAR can be demonstrated with the known f_s and f_p :

$$k_{\text{eff}}^2 = \frac{\left(f_p^2 - f_s^2\right)}{f_p^2} \cong 2 \cdot \frac{\left(f_p - f_s\right)}{f_p}. \quad (8)$$

Based on the definition published in the IEEE Std. 176-1987 [17], f_s is the frequency corresponding with the maximum conductance. Then f_s can be calculated by (7), and k_{eff}^2 can be evaluated by (8). However, k_{eff}^2 is not only determined by k_t^2 but also closely related with the electrode and resonator structure.

In the calculation of the resonance frequency f_s with (7), the dielectric, the piezoelectric, and the elastic constants of the piezoelectric film and the elastic constants of the electrodes generally are complex values, but all others, such as k_t^2, are considered as real values [12]. In addition, for a given piezofilm, C_0 is a constant. The complex velocity $\widetilde{V}_l$ in piezofilms or electrodes was given by a complex expression [12]

$$\widetilde{V} = \left[\frac{\left(C_{33}' + jC_{33}''\right)}{\rho}\right]^{1/2} \cong V'\left[1 + \frac{j}{(2Q_m)}\right]. \quad (9)$$

$V' = \sqrt{C_{33}'/\rho}$ is the real part, $V'' = \sqrt{C_{33}''/\rho}$ is the imaginary part, and C_{33}' and C_{33}'' are the real part and imaginary part of elastic constant C_{33}, where C_{33}'' is responsible for the mechanical losses, and $Q_m = C'/C'' \cong V'/2V''$ is the mechanical quality factor of the piezofilm or the electrode.

So the resonance frequency and the effective electromechanical coupling coefficient of FBAR can be obtained and analyzed by above definitions and equations.

3. Effects of Material Quality Factors on Effective Coupling Factor

The effect of electrode on FBAR performance is studied and shown in the following parts, and the thickness, d_e, the density, ρ_e, on the resonance frequency, f_s, and the effective electromechanical coupling factor, k_{eff}^2, are investigated; besides, the acoustic velocity v_e on k_{eff}^2 is also done. The different piezoelectric films of ZnO and AlN with thickness of 2 μm are used in this research, and they both are typical examples in the realistic applications, and the constants of material used in the calculation are shown in Table 1.

3.1. Effects of ρ_e and d_e on f_s of FBAR. The resonance frequency is very important parameter for frequency devices, especially for the acoustic device with vibration such as FBAR. In general, the frequency of FBAR is the basic parameter which should be considered during the design of FBAR, and so it is why we began with it.

Table 1: Data of material properties.

Material	Density (kg/m^3)	Velocity (m/s)	Impedance ($10^6\ \text{kg/m}^3\text{s}$)	k_t^2
ZnO	5606	6350	35.6	7.50
AlN	3300	11050	36.5	6.25

The resonance frequency definitions are stated in the IEEE Std. 176-1987 that f_s is defined as the frequency of maximum conductance [17]. So we can calculate f_s by setting the conductance maximum with (7). In the calculations, we take the different piezoelectric films with ZnO and AlN and take all other parameters as constants except the density and the thickness of electrode. We can take the different density as different electrode material and study what will happen to the resonance frequency of FBAR if we change the thickness of the same material electrode, which is very valuable for the design of FBAR devices.

The results of f_s changing with ρ_e and d_e of FBAR based on ZnO and AlN piezoelectric films were obtained, and the three-dimensional (3D) figures were shown as Figures 3(a) and 4(a), respectively, and the two-dimensional (2D) figures were shown as Figures 3(b) and 4(b), respectively. It can be obtained that the resonance frequency decreases with the thickness and the density of electrode increasing by the 3D figures, and this rule becomes more typical with the thin electrode or the high density, and it is the most obvious when both thickness and density of electrode appear in large value area. So we can choose proper material with small density and thin electrode for high resonance frequency by these results even though there still are some other parameters which should also be considered such as acoustic velocity. However, if the acoustic velocity in the electrode is a constant, then this result can be effectively used to design and evaluate the resonance frequency according to the application requirement. The above results can also be proved by the two 2D figures. Besides, we also can get that the FBAR decreased over half of resonance frequency just with the thickness change of 0.4 μm, and so the thickness effect of electrode on the resonance frequency are very distinct, which becomes smoother in the smaller thickness area.

3.2. Effects of ρ_e and d_e on k_{eff}^2 of FBAR. Based on the definition published in the IEEE Std. 176-1987 [17], f_s is the frequency of maximum conductance and f_p is the frequency of maximum resistance. Then f_s and f_p can be calculated by (7), and k_{eff}^2 can be evaluated by (8). k_{eff}^2 is not only determined by k_t^2 but also determined by the electrode and resonator structure.

We calculated k_{eff}^2 changing with the thickness and the density of electrode, and the 3D figures and 2D figures were given in Figures 5 and 6 with ZnO and AlN piezoelectric films, respectively.

It can be obtained by Figures 5(a) and 6(a) that there is the maximum k_{eff}^2 corresponding to some compositions of thickness and density of electrode, which is near the thin electrode and high density area. k_{eff}^2 increases and then

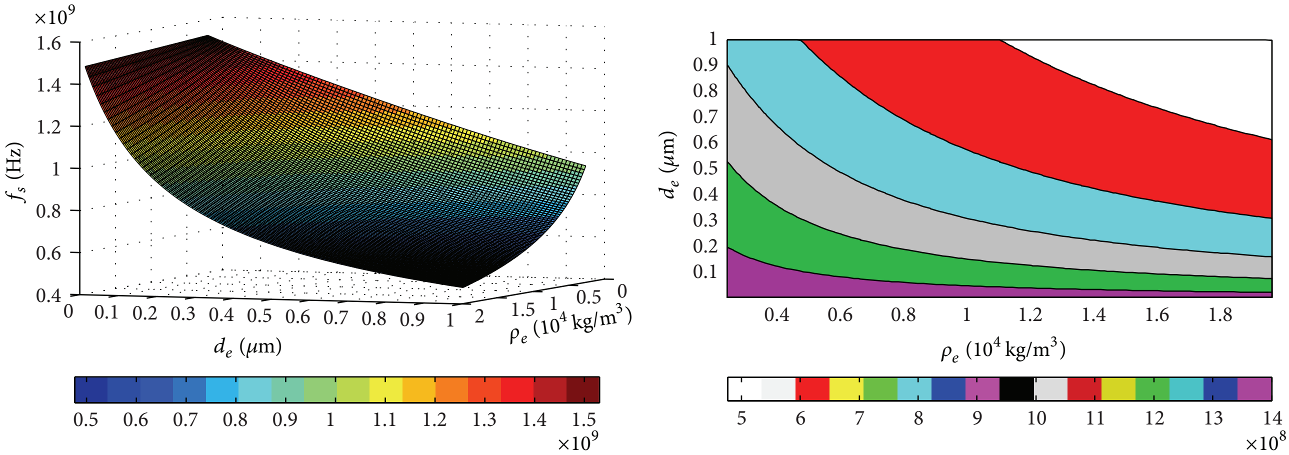

(a) (b)

FIGURE 3: f_s of FBAR versus the thickness and the density of electrode with ZnO piezoelectric film.

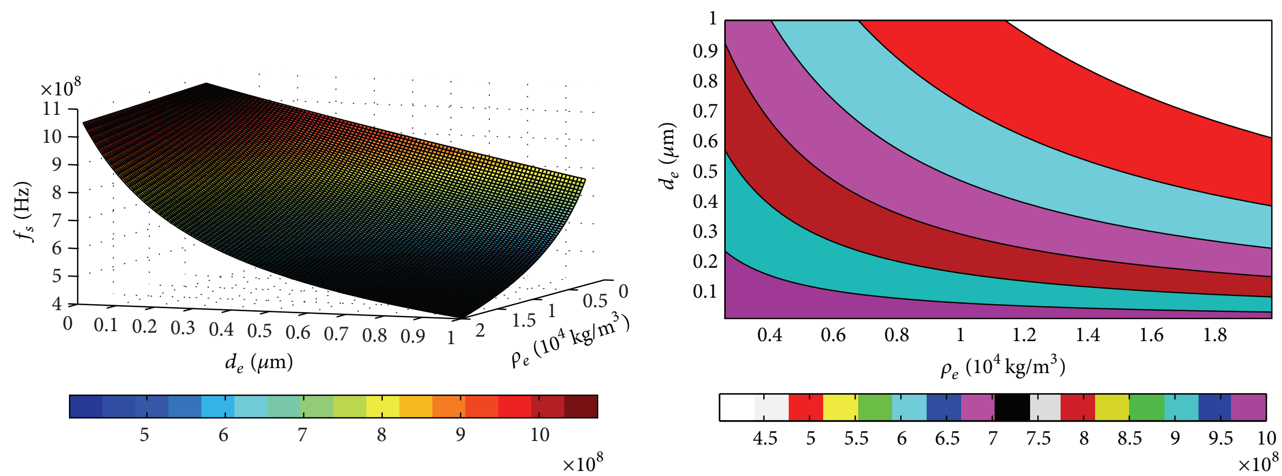

(a) (b)

FIGURE 4: f_s of FBAR versus the thickness and the density of electrode with AlN piezoelectric film.

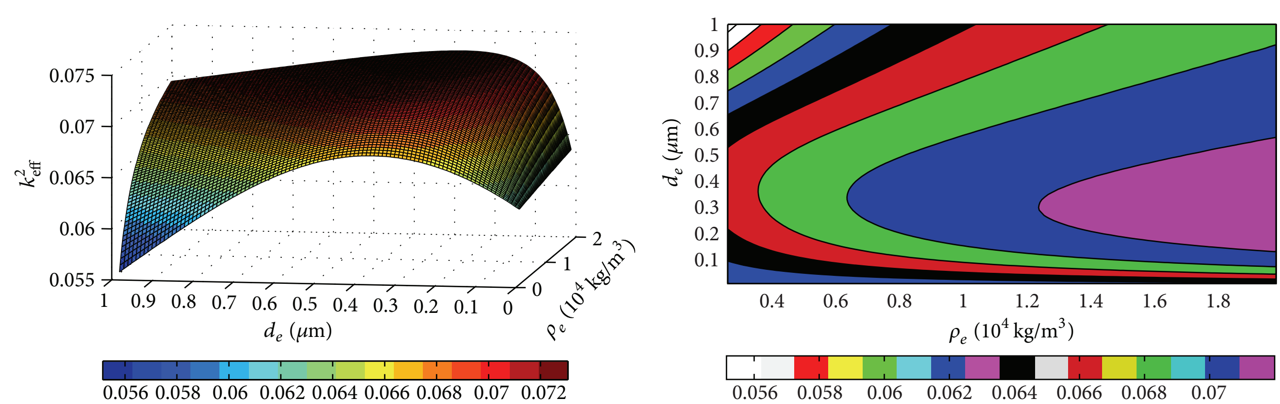

(a) (b)

FIGURE 5: k^2_{eff} of FBAR versus the thickness and the density of electrode with ZnO piezoelectric film.

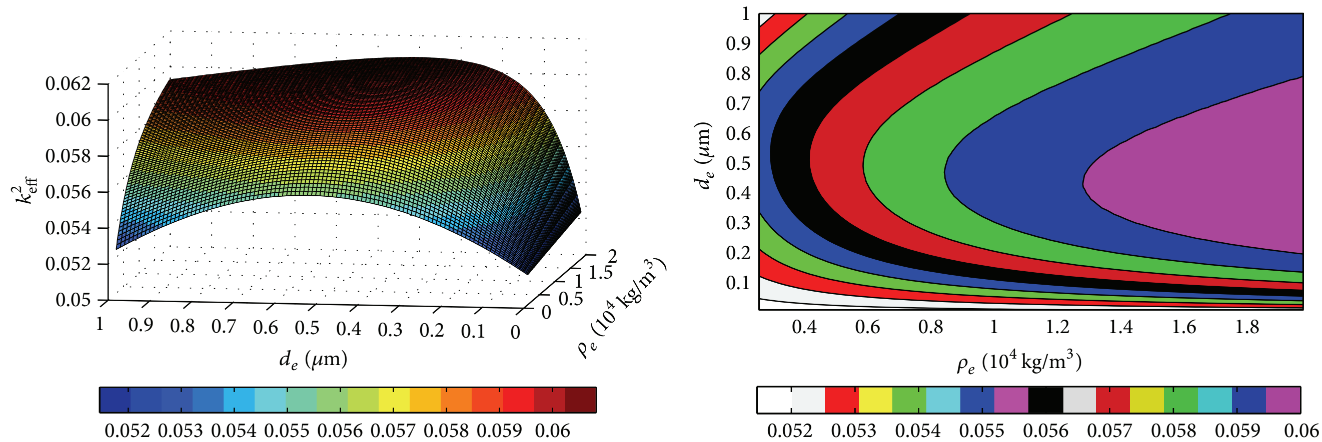

(a) (b)

FIGURE 6: k_{eff}^2 of FBAR versus the thickness and the density of electrode with AlN piezoelectric film.

decreases with the thickness increasing, and the increasing ratio can reach to 20% over original value of piezoelectric film. However, k_{eff}^2 mostly increases with the density of electrode. k_{eff}^2 changes fast with the thickness of electrode when the density of electrode is small, and vice versa. The FBAR with the ZnO layer shows that k_{eff}^2 changes more quickly than the case of AlN, and the thickness effect is more obvious too, especially for the small density of electrode cases. Furthermore, we can also get the same witness from the 2D figures of Figures 5(b) and 6(b).

A very interesting result is obtained from 2D figures that k_{eff}^2 will arrive at a maximum area with special thickness values for any density of electrode, and the corresponding thickness area is very obvious at the center, such as the FBAR with ZnO. The thickness beginning with the maximum k_{eff}^2 area is nearby 0.37 μm, and the thickness is nearby 0.5 μm for the AlN case. This is a very interesting and important result, and it means the effect of thickness on k_{eff}^2 has a strong rule which is affected little by the density of electrode material. We analyzed this phenomenon that it is the thickness where standing wave appears, and the difference between these two piezoelectric film cases should be attributed to the different piezoelectric thin films. Moreover, it confirms that the standing wave exists in the FBAR, and the thickness of electrode should be optimized with this merit point, which is effective for all kinds of electrode materials.

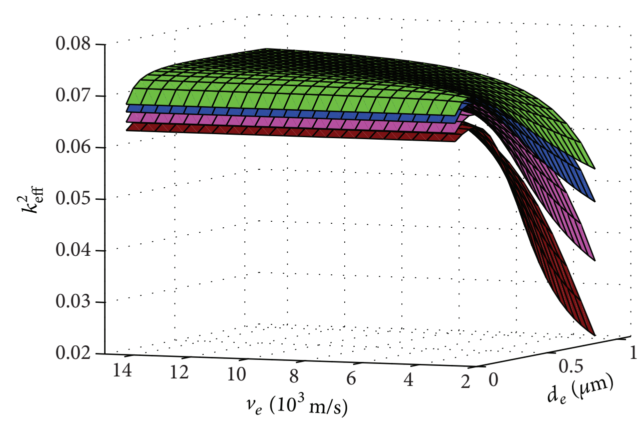

Number 1: $\rho_e = 1.9 \times 10^4$ kg/m^3 max k = 0.074156 ($v_e = 14.5 \times 10^3$ m/s, $d_e = 0.55\,\mu$m)

Number 2: $\rho_e = 1.3 \times 10^4$ kg/m^3 max k = 0.07372 ($v_e = 14.5 \times 10^3$ m/s, $d_e = 0.6\,\mu$m)

Number 3: $\rho_e = 7 \times 10^3$ kg/m^3 max k = 0.072642 ($v_e = 14.5 \times 10^3$ m/s, $d_e = 0.65\,\mu$m)

Number 4: $\rho_e = 2 \times 10^3$ kg/m^3 max k = 0.07028 ($v_e = 14.5 \times 10^3$ m/s, $d_e = 0.8\,\mu$m)

FIGURE 7: k_{eff}^2 of FBAR versus the thickness and the acoustic velocity of electrode with ZnO piezoelectric film and different density (3D curves).

3.3. Effects of v_e and d_e on k_{eff}^2 of FBAR. For overall evaluation of k_{eff}^2, the effects of v_e and d_e on k_{eff}^2 were conducted with the 2 μm thick piezoelectric film, and the 2D and 3D figures with four different electrode density choices were given for contrasting. The 3D k_{eff}^2 versus v_e and d_e curves based on ZnO and AlN were shown in Figures 7 and 9, respectively, and the 2D results were shown in Figures 8 and 10 correspondingly. The key parameters and results were marked on the 3D figures. We can get that k_{eff}^2 always rises with the density of electrode for the ZnO case in Figure 7 which also can be observed in above section results, and the maximum k_{eff}^2 always appears at the maximum acoustic velocity during our calculation range. The AlN case is the same behavior as the ZnO FBAR in Figure 9. Moreover, k_{eff}^2 rises more obviously with v_e in the large electrode thickness area and vice versa, and k_{eff}^2 changes little with v_e among the small electrode thickness area and especially least in the high density electrode material area. On the other hand, k_{eff}^2 rises distinctly with the electrode thickness in the low velocity area, but it almost does not change in the high velocity space.

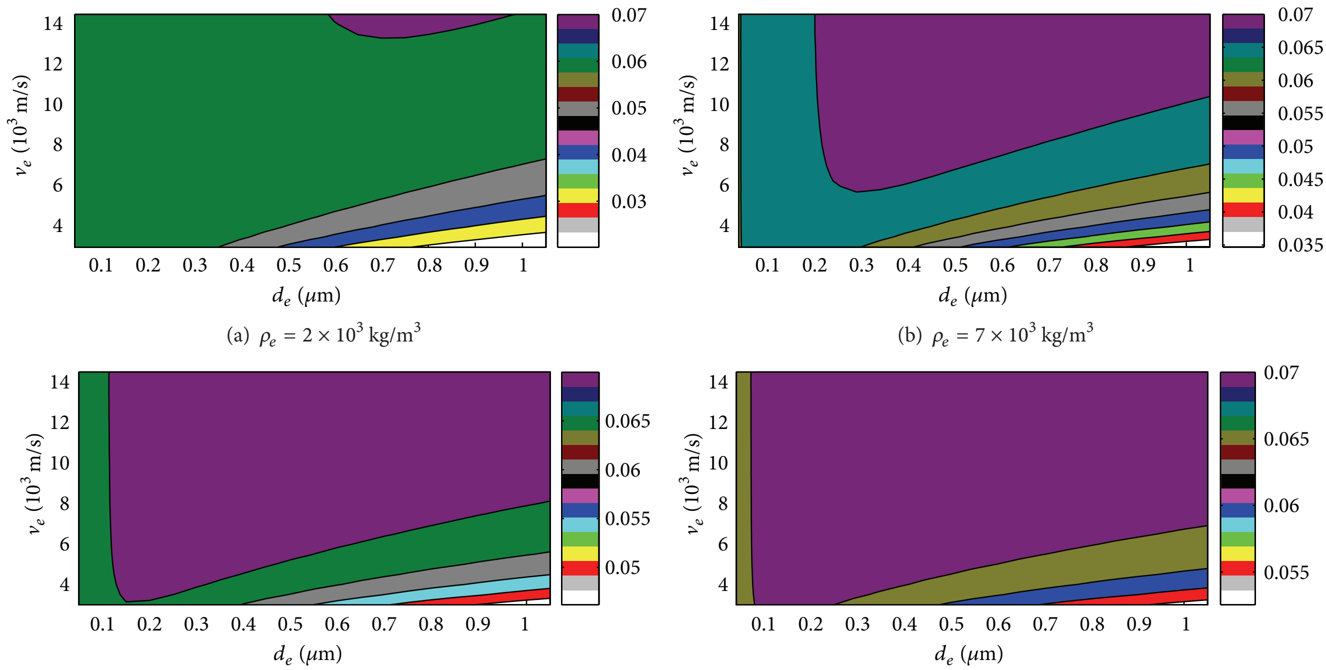

(a) $\rho_e = 2 \times 10^3$ kg/m^3 (b) $\rho_e = 7 \times 10^3$ kg/m^3

(c) $\rho_e = 1.3 \times 10^4$ kg/m^3 (d) $\rho_e = 1.9 \times 10^4$ kg/m^3

Figure 8: k_{eff}^2 of FBAR versus the thickness and the acoustic velocity of electrode with ZnO piezoelectric film (2D curves).

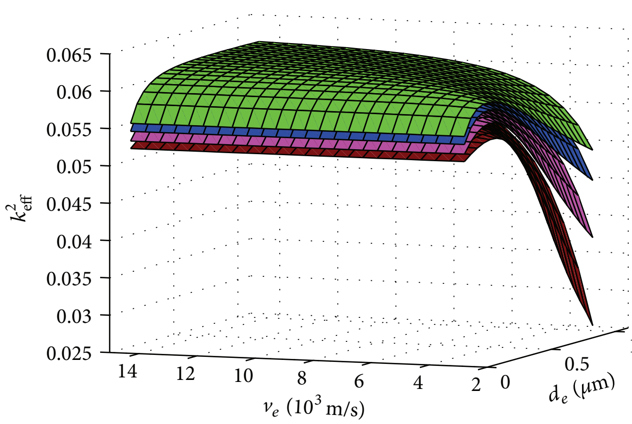

Number 1: $\rho_e = 1.9 \times 10^4$ kg/m^3 max $k = 0.061766$ ($v_e = 14.5 \times 10^3$ m/s, $d_e = 0.8\,\mu$m)

Number 2: $\rho_e = 1.3 \times 10^4$ kg/m^3 max $k = 0.061397$ ($v_e = 14.5 \times 10^3$ m/s, $d_e = 0.9\,\mu$m)

Number 3: $\rho_e = 7 \times 10^3$ kg/m^3 max $k = 0.060458$ ($v_e = 14.5 \times 10^3$ m/s, $d_e = 0.95\,\mu$m)

Number 4: $\rho_e = 2 \times 10^3$ kg/m^3 max $k = 0.058439$ ($v_e = 14.5 \times 10^3$ m/s, $d_e = 1.05\,\mu$m)

Figure 9: k_{eff}^2 of FBAR versus the thickness and the acoustic velocity of electrode with AlN piezoelectric film and different density (3D curves).

We can conclude that k_{eff}^2 is in the direct proportion to the density ρ_e here, and the acoustic velocity of electrode has a similar effect too, and k_{eff}^2 dominantly rises with v_e. The electrode thickness affects small k_{eff}^2 with high v_e; moreover, when v_e is high enough, then k_{eff}^2 has almost nothing to do with d_e. But k_{eff}^2 changes fast with d_e when v_e is small, and k_{eff}^2 rises with electrode thickness first and then descends with its rising, which was also observed in the former section. The thickness corresponding to the maximum k_{eff}^2 is different with different electrode density; however, it descends with density ascending, which also proves the special value $\rho_e d_e$ corresponding with the maximum k_{eff}^2 of FBAR even though we cannot get this result directly by these figures because there are not so many piezoelectric film parameters considered for proving [14]. All these behaviors are similar for both ZnO and AlN based FBARs.

The density, acoustic velocity, and thickness of electrode of FBAR can be optimized by above results for special f_s and k_{eff}^2 need. We can get the higher k_{eff}^2 with the higher electrode density, and it is also the same to acoustic velocity of electrode material. The best thickness of electrode is decided by density and especially acoustic velocity; however, the thickness effects are obvious when the acoustic velocity is small, but it almost does not change if the acoustic velocity is very big. Moreover, the best thickness corresponding to the maximum k_{eff}^2 is different with different cases, but the values are in the special area comparing with the distinctly variable v_e and ρ_e, and it is because we take most of the parameters of piezoelectric thin film as constants, even though these results can be observed in both ZnO and AlN FBARs in this research.

4. Conclusions

In this paper, the following research and results have been given.

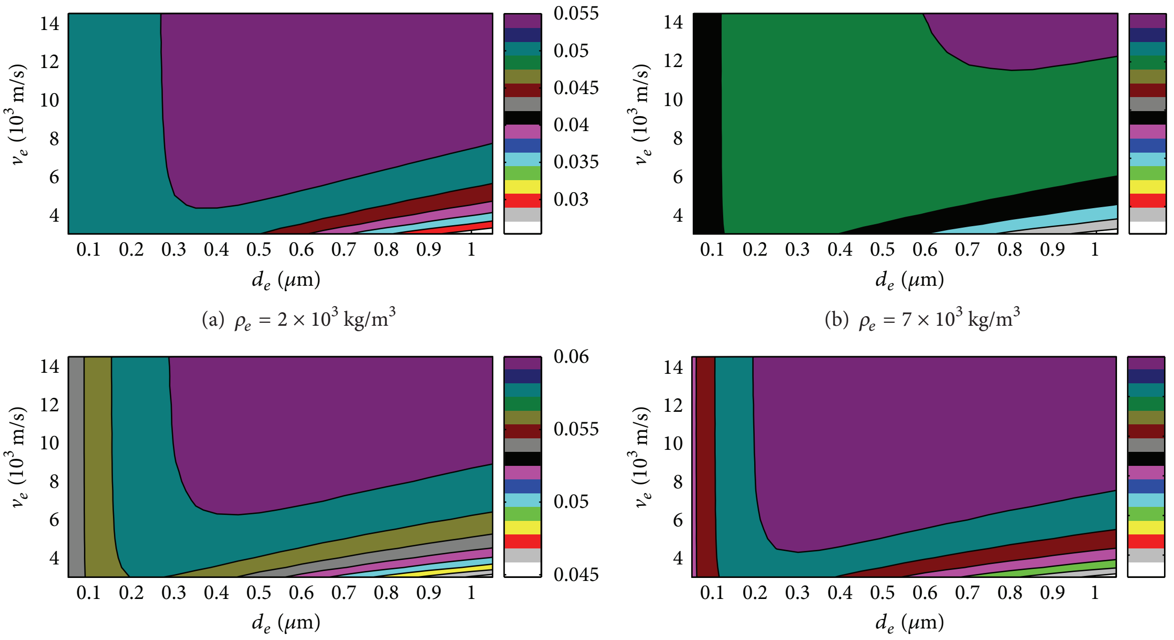

(a) $\rho_e = 2 \times 10^3$ kg/m^3 (b) $\rho_e = 7 \times 10^3$ kg/m^3 (c) $\rho_e = 1.3 \times 10^4$ kg/m^3 (d) $\rho_e = 1.9 \times 10^4$ kg/m^3

FIGURE 10: k_{eff}^2 of FBAR versus the thickness and the acoustic velocity of electrode with AlN piezoelectric film and different density (2D curves).

(i) Firstly, we derived the input acoustic impedance equation with transfer matrix method, and the simplified impedance equation of FBAR with the same top and bottom electrode is obtained. This equation can be applied extensively to calculate the resonance frequency, the effective electromechanical coupling factor, the mechanical quality factor, and the merit figure of FBAR, which makes the theoretical calculation and optimization easy.

(ii) Secondly, the effect of thickness and density of electrode on the resonance frequency of FBAR was investigated, and it can be obtained that the thickness and the density of electrode affect the resonance frequency obviously, especially at the large thickness and density area. This result shows that the thickness and the material of electrode are very key parameters for the resonance frequency design of FBAR.

(iii) Finally, the effects of thickness, density, and acoustic velocity on the effective electromechanical coupling factor were studied, respectively. The results show that k_{eff}^2 is in the direct proportion to both density ρ_e and v_e of electrode. The electrode thickness affects small k_{eff}^2 with high v_e; moreover, when v_e is high enough, then k_{eff}^2 has almost nothing to do with d_e. k_{eff}^2 rises with electrode thickness first and then descends with its rising, and the thickness corresponding to the maximum k_{eff}^2 is different with different electrode density and v_e, but they almost locate in the special area.

All above results indicate that the thickness, density, and acoustic velocity of electrode are very important, and they can be applied to optimize and design different kind of FBARs.

Conflict of Interests

The authors declare that there is no conflict of interests regarding the publication of this paper.

Acknowledgments

This work is supported by the National Natural Science Foundation of China (nos. 61201088, 11404257, and 11504291), Shaanxi Province Innovation Project for Science and Technology Overall Planning (no. 2012KTCL01-12), Industrialization Foundation of Shaanxi Educational Committee (no. 2011JG10), and Xi'an Technology Transferring and Promoting Project (CXY1342(5), CX1253(2)).

References

[1] J. D. Larson III, R. Ruby, P. Bradley, and Y. Oshmyansky, "BAW antenna duplex for the 1900 MHz PCS band," in *Proceedings of the IEEE Ultrasonics Symposium*, pp. 887–890, Caesars Tahoe, NV, USA, October 1999.

[2] R. Ruby, P. Bradley, J. D. Larson III, and Y. Oshmyansky, "PCS 1900 MHz duplexer using thin film bulk acoustic resonators (FBARs)," *Electronics Letters*, vol. 35, no. 10, pp. 794–796, 1999.

[3] R. C. Ruby, P. Bradley, Y. Oshmyansky, A. Chien, and J. D. Larson III, "Thin film bulk wave acoustic resonators (FBAR) for wireless applications," in *Proceedings of the Ultrasonics Symposium*, pp. 813–821, October 2001.

[4] K. M. Lakin, J. Belsick, J. F. McDonald, and K. T. McCarron, "Improved bulk wave resonator coupling coefficient for wide bandwidth filters," in *Proceedings of the IEEE Ultrasonics Symposium*, vol. 1, pp. 827–831, IEEE, Atlanta, Ga, USA, October 2001.

[5] I. Voiculescu and A. N. Nordin, "Acoustic wave based MEMS devices for biosensing applications," *Biosensors and Bioelectronics*, vol. 33, no. 1, pp. 1–9, 2012.

[6] F. T. Chu, C. Li, Z. Z. Wang, and X. Z. Liu, "Aluminum Nitride Thin films on molybdenum/polyimide heterostructure for bulk acoustic resonators," *Rare Metal Materials and Engineering*, vol. 42, no. 10, pp. 2023–2026, 2013.

[7] A. J. Festschrift, J. K. Luo, Y. Q. Fu et al., "ZnO based SAW and FBAR devices for bio-sensing applications," *Journal of Non-Newtonian Fluid Mechanics*, vol. 222, pp. 209–216, 2015.

[8] H. Zhang, G. Jiang, Z. Liu, S. Zhang, and L. Fan, "Optimizations of composited acoustic sensors with a microfluidic channel," *Journal of Applied Physics*, vol. 115, no. 13, Article ID 133502, 2014.

[9] A. Vorobiev and S. Gevorgian, "Intrinsically switchable thin film bulk acoustic wave resonators," *Applied Physics Letters*, vol. 104, no. 22, Article ID 222905, 2014.

[10] H. J. Lee, K. A. Hyun, and H. I. Jung, "A high-Q resonator using biocompatible materials at microwave frequencies," *Applied Physics Letters*, vol. 104, no. 2, Article ID 023509, 2014.

[11] M.-C. Chao, Z.-N. Huang, S.-Y. Pao, Z. Wang, and C. S. Lam, "Modified BVD-equivalent circuit of FBAR by taking electrodes into account," in *Proceedings of the IEEE Ultrasonics Symposium*, pp. 973–976, October 2002.

[12] Q. Chen and Q.-M. Wang, "The effective electromechanical coupling coefficient of piezoelectric thin-film resonators," *Applied Physics Letters*, vol. 86, no. 2, Article ID 022904, 2005.

[13] Y. Zhang, Z. Wang, and J. D. N. Cheeke, "Resonant spectrum method to characterize piezoelectric films in composite resonators," *IEEE Transactions on Ultrasonics, Ferroelectrics, and Frequency Control*, vol. 50, no. 3, pp. 321–333, 2003.

[14] T. Zhang, H. Zhang, Z.-Q. Wang, and S.-Y. Zhang, "Effects of electrodes on performance figures of thin film bulk acoustic resonators," *Journal of the Acoustical Society of America*, vol. 122, no. 3, pp. 1646–1651, 2007.

[15] N. F. Naumenko, "Advanced numerical technique for analysis of surface and bulk acoustic waves in resonators using periodic metal gratings," *Journal of Applied Physics*, vol. 116, no. 10, Article ID 104503, 2014.

[16] A. Kvasov and A. K. Tagantsev, "Thin film bulk acoustic wave resonators tuning from first principles," *Journal of Applied Physics*, vol. 113, no. 20, Article ID 204104, 2013.

[17] IEEE, "IEEE standard on piezoelectricity," Tech. Rep. 176-1987, IEEE Transactions on Ultrasonics, Ferroelectrics and Frequency Control, 1996, 43:719.